

THE HIGH-CURRENT ELECTRON BEAM TRANSPORT EXPERIMENT AT THE UNIVERSITY OF MARYLAND*

M. Reiser, E. Chojnacki, P. Loschialpo, and W. Namkung
 Laboratory for Plasma and Fusion Energy Studies
 University of Maryland
 College Park, Maryland 20742 U.S.A.

J. D. Lawson, C. Prior, and G. P. Warner
 Rutherford-Appleton Laboratory
 Chilton, Oxon
 United Kingdom

Summary

The status of the electron beam transport experiment at the University of Maryland is reviewed. Beam transport studies in the first stage of twelve solenoid lenses have been completed, and 100% current transmission with very little emittance change was measured for the parameter range $40^\circ < \sigma_0 < 110^\circ$. The channel is now being extended to its full design length of 36 lenses.

Introduction

The electron beam transport experiment at the University of Maryland has been designed to study the effects that limit the beam current and increase the emittance in a periodic focusing channel. Theoretical considerations, design features, and results of studies with one or two single solenoid lenses were reported in several previous papers.¹⁻⁴ Last year, the first stage of the periodic channel consisting of 12 short solenoid lenses was completed, and detailed measurements of beam transmission and emittance were made.⁵ Construction of Stage 2 in which the channel is extended to its full length of 36 lenses is in progress, and experiments with the completed transport system should begin in late summer of this year.

In parallel with the work on the periodic transport channel, two separate studies on special problems relating to the goals of our project were conducted. The first study, at the Rutherford-Appleton Laboratory, was concerned with the use of special grids to increase the beam emittance and thereby extend the region of parameter space in the experiment. Results of this work were reported in Ref. 4. The second study, at the University of Maryland, involved a methodical investigation of the effects of lens aberrations and space charge forces on the focusing of an electron beam by a single lens.^{6,7}

Below, we will present a brief summary of the major results of the transport experiments in the 12-lens channel stage and of the single-lens studies on aberrations and space charge effects. The details concerning this work can be found in Refs. 5-7.

Beam Transport Results in 12-Lens Channel

The experimental arrangement of the electron beam transport channel is shown schematically in Fig. 1. The electron gun used in these studies has a cathode radius of 1.27 cm and typical operating conditions were 5 kV, 220 mA, 5 μ s pulse length (to avoid space charge neutralization) and 60 Hz repetition rate. Downstream from the gun are two solenoids, M1 and M2, that are used for matching the beam into the channel of periodically spaced lenses, C1 to C12 (length of one period is 13.6 cm). Short diagnostic ports are provided between lenses M2 and C1 and C6 and C7. The main diagnostic chamber with current monitor (Rogowski coil), fluorescent screen, a slit/Faraday cup system, and a "pepperpot" mask--both for emittance measurements--is located at the end of the channel. The fluorescent screen can be moved a short distance into the channel, and the beam spot on the screen can

be viewed or photographed through a viewing port at the rear.

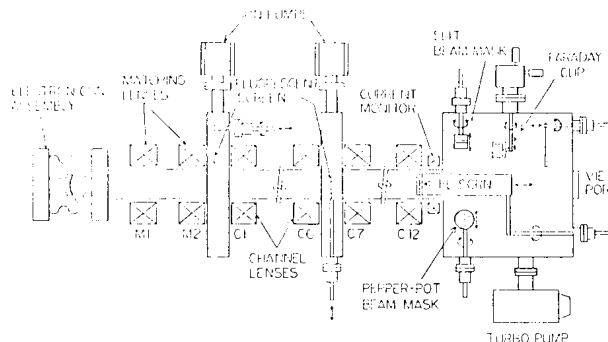


FIG. 1. Schematic of the University of Maryland Beam Transport Experiment.

The unnormalized intrinsic RMS emittance due to the cathode temperature T is given by the formula $\bar{\epsilon} = R_c [2kT/eV]^{1/2}$, where R_c is the cathode radius and V the accelerating voltage of the gun. For $V = 5$ kV, $R_c = 1.27$ cm, and $kT = 0.13$ eV, one gets $\bar{\epsilon} = 9.2 \times 10^{-5}$ m-rad, or $\epsilon_N = \beta\gamma\bar{\epsilon} = 1.3 \times 10^{-5}$ m-rad for the normalized emittance. The generalized perveance is $K = (I/I_0)(2/\beta^3\gamma^3)$, with $I_0 = 4\pi\epsilon_0 m_0 c^3/e = 1.7 \times 10^4$ Amps for electrons; for $I = 220$ mA, $V = 5$ kV, one obtains $K = 9.358 \times 10^{-3}$. According to the smooth-approximation theory, the ratio of σ to σ_0 , the phase shifts with space charge and without space charge, in a channel with period S is given by $\sigma/\sigma_0 = [1 + u^2]^{1/2} - u$, where $u = Ks/(2\sigma_0\epsilon)$. For our experiment, taking the above value of the intrinsic emittance and $S = 0.136$ m, one finds $u = 6.314$, $\sigma/\sigma_0 = 0.079$ for $\sigma_0 = 60^\circ$ and $u = 4.403$, $\sigma/\sigma_0 = 0.112$ for $\sigma_0 = 90^\circ$. Thus, we are operating in a space-charge dominated regime very close to the laminar-flow limit ($\sigma/\sigma_0 \rightarrow 0$). For matched conditions, the beam radius has a maximum, R_{max} , at the center of each lens and a minimum, R_{min} , at the center of the drift space between lenses. Figure 2 shows the calculated theoretical values for R_{max} and R_{min} as a function of σ_0 which in turn depends on the magnetic field strength of the lenses. These curves were obtained by integrating the K-V envelope equations using the parameter values given above. We note that the K-V equations included only the linear force terms of the applied field and the space charge. As indicated in the figure, the maximum beam radius exceeds the tube radius when $\sigma_0 < 40^\circ$. As σ_0 increases, the two radii decrease rapidly and then, above $\sigma_0 = 120^\circ$, begin to level off. Simultaneously, the ripple $\Delta R/R$ increases significantly with larger values of σ_0 .

Beam matching was accomplished experimentally by varying the field strength in coils M1 and M2 until maximum current transmission was obtained with best beam quality. The measured beam transmission efficiency through the 12-lens channel as a function of σ_0 is plotted in Fig. 3. There is 100% transmission

*Supported by United States Department of Energy.

efficiency over the range $40^\circ < \sigma < 110^\circ$. The decrease of transported current below $\sigma = 40^\circ$ is due to the fact that the beam hits the wall of the tube, in agreement with theoretical expectations (see Fig. 2). The rapid drop above $\sigma = 110^\circ$ is due to "halo" formation which results in beam loss to the wall. However, the behavior of the beam in that region is only of academic interest since in a practical channel one operates at, or below, $\sigma = 90^\circ$ to avoid the envelope instabilities predicted by theory.⁹ It should be noted in this context that we do not expect to see the third-order instability in the few periods of our channel. Theoretical studies with different beam phase-space distributions¹⁰ and the experimental results at Berkeley¹¹ indicate that this instability may not be very noticeable in quadrupole channels. From the theory, it is known that the growth rate and instability region is considerably smaller in a solenoid than in a quadrupole system, and I. Haber found no evidence of RMS emittance growth in recent simulation studies.¹²

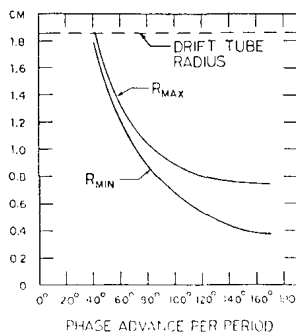


FIG. 2. Maximum and minimum envelope radius versus σ for a K-V beam (5 KeV, 220 mA, $\bar{\epsilon} = 9.2 \times 10^{-5}$ m-rad).

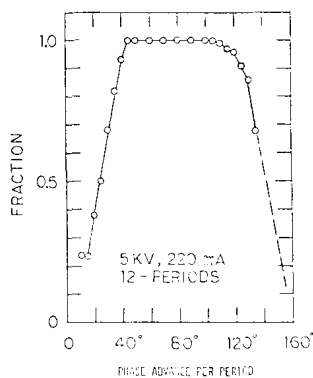


FIG. 3. The measured fraction of the 5 KeV, 220 mA beam transported through the 12-period channel versus the phase advance per period σ .

In Fig. 4, we show measurements of the beam radius in the last two lens sections of our channel using the movable fluorescent screen. At $\sigma = 60^\circ$, the measured radius is about 10% smaller than the theoretical curve obtained from the K-V envelope equation. We attribute this difference to the effects of the nonlinear lens fields which increase the net focusing forces, as will be discussed in the next section. At $\sigma = 90^\circ$, the measurements are in better agreement with the theoretical curve.

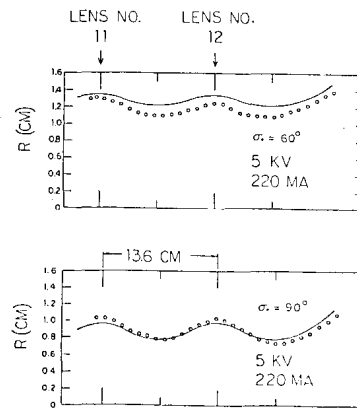


FIG. 4. Beam envelope at the end of 12-lens solenoid transport channel for $\sigma = 60^\circ$, $\sigma = 4.5^\circ$ (upper figure) and $\sigma = 90^\circ$, $\sigma = 10^\circ$ (lower figure). The solid curve represents the calculated matched-beam envelope for a K-V distribution; the circles represent experimental data.

Emittance measurements were made using a slit and pinhole/Faraday cup method as discussed in Ref. 5. The results obtained by evaluating the experimental data are summarized in Table I. On top we listed the intrinsic theoretical value for the RMS emittance. Below it is the value measured before the beam was injected into the solenoid system; it is remarkably close to this theoretical limit. The measurements at the end of the 12-lens channel show a relatively small emittance growth of about 30% which decreases slightly as σ is varied from 60° to 90° . We suspect that this growth is due to lens aberrations and space charge effects and hope that numerical simulation studies in the future will clarify this question.

TABLE I. RMS emittance data in 10^{-5} m-rad.

Intrinsic Theoretical Emittance	9.2
Measured Emittance Before Channel Entrance	10.3
Measured Emittance at the End of 12-Lens Channel:	
$\sigma = 60^\circ$	13.1
$\sigma = 70^\circ$	13.0
$\sigma = 90^\circ$	12.7

Effects of Nonlinear Focusing Forces and Space Charge in a Single Lens

The ideal case of a uniform beam in a linear focusing system is described by the well-known K-V equations. When the nonlinear terms of the focusing forces are taken into account, the trajectories are changed and an initially uniform charge distribution becomes nonuniform. These effects were studied in an experiment with a single solenoid lens.^{6,7} The measured magnetic field on the axis of the solenoid can be approximated rather accurately by the analytical formula

$$B(z) = B_0 [1 + (z/a)^2]^{-1} \exp[-(z/d)^2] \quad (1)$$

where $d = 3.24$ cm and $a = 4.40$ cm. The trajectory equation can be written in the form^{4,6}

$$r'' + \sum_{i=0}^4 F_i - \frac{KF_s}{r} = 0 \quad (2)$$

where $F_0 = \kappa r = [eB(z)/2\gamma m\beta c]^2 r$ represents the linear focusing force, F_1 to F_4 the third-order terms of the focusing field, and KF_s/r the space charge effects (F_s is a function of r in general). The ratios of the nonlinear to the linear force terms are given in Table II below. To obtain a rough idea of the relative strength, these ratios have been evaluated for our solenoid in the thin-lens limit ($r = \text{const.}$) using Eq. (1) for $B(z)$ and its derivatives, $B'(z)$ and $B''(z)$. For this calculation, it was assumed that the trajectory is parallel to the axis (i.e. $r' = 0$) before entering the lens field. The results are shown in the last column of the table. Note that κ is proportional to the square of the peak solenoidal field, B_0 , which in the single-lens experiment (as well as in the channel transport studies) was varied, typically, between 70 and 130 G. For a 5 keV electron beam ($\beta\gamma = 0.14$) and $B_0 = 100$ G, $\kappa = 4.39 \times 10^{-2} \text{ cm}^{-2}$, and the corresponding thin-lens values for the four nonlinear terms are shown in the last column. From the table, we see that all third-order forces except F_3 have a net focusing effect (positive sign). By far the most important term is F_4 which results from the fact that the axial field $B_z(r,z) = B(z) - 0.25 B''(z)r^2$ increases with radius since $B''(z)$ is predominantly negative within the lens region. F_4 is independent of B_0 in this approximation. The first term (F_1) on the other hand, is proportional to B_0^2 , but at $B_0 = 100$ G its value is only about 10% of the magnitude of F_4/F_0 . The electron beam radius in the single-lens experiment (as well as in the channel studies) varied typically between about 0.8 cm and 1.8 cm. Thus, the dominant third-order term F_4/F_0 increases the net focusing force at the edge of the beam by 6% to 31%, respectively. In the periodic channel, the maximum radius of the matched beam at $\sigma = 60^\circ$ is about 1.4 cm, according to Fig. 2. This corresponds to $F_4/F_0 = 0.19$, i.e. an increase of the single-lens focusing effect of about 19% in the above approximation. We believe that this increase of the focusing strength due to the nonlinear force terms explains the smaller beam radius observed in the channel studies for $\sigma = 60^\circ$ and the much better agreement with linear theory at $\sigma_0 = 90^\circ$ (where $r \approx 0.95$ cm, $F_4/F_0 \approx 0.09$).

TABLE II. Ratio of nonlinear force terms to linear force. In the third column, κ_0 and r are in units of cm^{-2} and cm, respectively.

Nonlinear Term	Analytical Form	Thin-Lens Approximation of $\int F_i dz / \int F_0 dz$	
		General Formula	$B_0 = 100$ G, $\beta\gamma = 0.14$
F_1/F_0	r'^2	$4.8 \kappa_0^2 r^2$	$0.009 r^2$
F_2/F_0	κr^2	$0.68 \kappa_0 r^2$	$0.030 r^2$
F_3/F_0	$-(B'/B)rr'$	$-0.48 \kappa_0 r^2$	$-0.021 r^2$
F_4/F_0	$-0.5(B''/B)r^2$	$0.097 r^2$	$0.097 r^2$

More accurate numerical integration of Eq. (2) shows that an initially uniform beam becomes hollow or sharply peaked after passage through the lens depending on the magnetic field strength. Comparison between theoretical results and measured beam profiles indicates remarkably good agreement.

These theoretical and experimental studies of beam focusing by a single solenoid are discussed in great detail in Refs. 6 and 7. The knowledge gained will be of great value in future studies of beam transport through the full periodic channel.

Conclusions and Future Plans

The main conclusions from our studies with the 12-lens channel are: (1) Beam transport with essentially no particle losses and with very little increase of the emittance ($\sim 30\%$) has been achieved over a range of $40^\circ < \sigma < 110^\circ$ at large tune depression of $\sigma/\sigma_0 \sim 0.1$, (2) There is no indication of any instability so far. The third-order mode is not expected to have any measurable effect--even in the longer channel of 36 lenses. Whether the beam loss at $\sigma > 110^\circ$ is due to nonlinear focusing effects of the type observed in our single-lens experiment or due to the predicted second-order ("envelope") instability remains to be investigated in the full channel. We hope to do computer simulation work that includes the nonlinear focusing forces for our channel--either at the Rutherford-Appleton Laboratory or with the collaboration of Dr. I. Haber, NRL.

Beyond the studies with the full solenoid channel, we are exploring possibilities to do longitudinal bunching/compression experiments. Such studies would be of great interest for heavy ion fusion and for bunch formation and initial acceleration in high-brightness linacs.

References

1. M. Reiser, W. Namkung, and M. A. Brennan, IEEE Trans. Nucl. Sci. **26**, 3026 (1979).
2. W. Namkung, M. Reiser, P. Loschialpo, M. Reiser, J. Suter, and J. D. Lawson, IEEE Trans. Nucl. Sci. **28**, 2519 (1981).
3. M. Reiser, W. Namkung, P. Loschialpo, J. Suter, and J. D. Lawson, Proc. of 1981 Linear Accelerator Conf., LA-9234-C, UC-28, issued Feb. 1982, p. 235.
4. J. D. Lawson, E. Chojnacki, P. Loschialpo, W. Namkung, C. R. Prior, T. C. Randle, D. H. Reading, and M. Reiser, IEEE Trans. Nucl. Sci. **30**, 2537 (1983).
5. E. Chojnacki, M.S. Thesis, University of Maryland, 1984.
6. P. Loschialpo, Ph.D. Thesis, University of Maryland, 1984.
7. P. Loschialpo, W. Namkung, M. Reiser, and J. D. Lawson, "Effects of Space Charge and Lens Aberrations in the Focusing of an Electron Beam by a Solenoid Lens," to be published.
8. M. Reiser, Part. Accel. **8**, 167 (1978).
9. I. Hofmann, L. J. Laslett, L. Smith, and I. Haber, Part. Accel. **13**, 145 (1984).
10. J. Struckmeier, J. Klabunde, and M. Reiser, "On the Stability of Different Particle Phase-Space Distributions in a Magnetic Quadrupole Channel," accepted for publication in Part. Accel.
11. See the paper on the Berkeley Beam Transport Experiment at this Conference.
12. I. Haber (private communication).